

# High temperature grown transition metal oxide thin films: tuning physical properties by MeV N<sup>+</sup>-ion bombardment

R Sivakumar<sup>1,5</sup>, C Sanjeeviraja<sup>2</sup>, M Jayachandran<sup>3</sup>, R Gopalakrishnan<sup>4</sup>,  
S N Sarangi<sup>1</sup>, D Paramanik<sup>1</sup> and T Som<sup>1,6</sup>

<sup>1</sup> Institute of Physics, Sachivalaya Marg, Bhubaneswar 751 005, India

<sup>2</sup> Department of Physics, Alagappa University, Karaikudi 630 003, India

<sup>3</sup> ECMS Division, Central Electrochemical Research Institute, Karaikudi 630 006, India

<sup>4</sup> Department of Physics, Anna University, Chennai 600 025, India

E-mail: [tsom@iopb.res.in](mailto:tsom@iopb.res.in)

Received 3 February 2008, in final form 6 April 2008

Published 29 May 2008

Online at [stacks.iop.org/JPhysD/41/125304](http://stacks.iop.org/JPhysD/41/125304)

## Abstract

In this paper, we present a systematic study on tuning the physical properties of high temperature (373 K) grown transition metal oxide thin films by the effect of 2 MeV nitrogen ion irradiation. Although we observe irradiation induced growth in crystallite sizes for both WO<sub>3</sub> and MoO<sub>3</sub> films, no structural phase change takes place in the films due to N<sup>+</sup>-ion beam irradiation even up to the fluence of  $1 \times 10^{15}$  N<sup>+</sup> cm<sup>-2</sup>. On the other hand, irradiation leads to a significant increase in the optical absorption and the surface roughness of the films. These observations are corroborated by micro-Raman analysis. The results are attributed to the MeV ion-matter interaction.

(Some figures in this article are in colour only in the electronic version)

## 1. Introduction

Due to their property of being chromogenic, the transition metal oxides have attracted much interest during the last two decades. Among the various transition metal oxides, tungsten oxide (WO<sub>3</sub>) and molybdenum oxide (MoO<sub>3</sub>) have been extensively considered by researchers owing to their remarkable applications in the fields of smart windows, solid-state micro-batteries, positive alpha-numeric display devices, photochromism and electrochromism [1–4]. However, the idea of altering the colour of selected materials by engineering their optical properties is a challenging task. Among the techniques devised to change the optical properties of transition metal oxides, electrochemical intercalation/deintercalation of alkali metal ions, namely H<sup>+</sup>, K<sup>+</sup> and Li<sup>+</sup>, appears to be popular. In this way the visible colour as well as the absorption behaviour in the infrared region can be reversibly switched and controlled by applying appropriate voltages [5, 6]. In

addition, WO<sub>3</sub> and/or MoO<sub>3</sub> can be coloured by exposing them to UV light, called photochromic effect, resulting in practically the same absorption band as for intercalation (electrochromic effect) [7]. In fact, creation of oxygen vacancies is the key to the coloration of transition metal oxides. Goulding *et al* [8] reported that the coloration of WO<sub>3</sub> films can be achieved by creating vacancies through thermochromic effect, i.e. by annealing WO<sub>3</sub> films beyond the temperature of 423 K. On the other hand, the coloration of MoO<sub>3</sub> film is obtained at an annealing temperature of 473 K [9].

Alternatively, vacancies can also be created in a solid by corresponding atomic displacements produced during energetic ion bombardment. In this process, ion irradiation helps to tailor different physical properties of materials with a high spatial selectivity [10]. There are some reports which show irradiation induced changes in electrical conductivity, optical refractive index and vibrational properties of WO<sub>3</sub> and MoO<sub>3</sub> films [11–15]. Generally, WO<sub>3</sub> and MoO<sub>3</sub> are insulators in their stoichiometric states at the ambient temperature due to the large energy band gap ( $E_g$ ) values. If coloured, however, by any of the above described chromogenic effects, the change

<sup>5</sup> Present address: Department of Electrical Engineering, Nagaoka University of Technology, 1603-1 Kamitomioka, Nagaoka, Niigata 940-2188, Japan.

<sup>6</sup> Author to whom any correspondence should be addressed.

in optical behaviour is accompanied by an increase in the electrical conductivity ( $\sigma$ ) over many orders of magnitude with a temperature dependence exhibiting Mott's law [ $\ln \sigma \propto T^{-1/4}$ ] indicating a variable range hopping conductivity [11]. In our recent works, we have reported the effects of  $N^+$ -ion irradiation on the change in optical energy band gap of electron beam evaporated  $WO_3$  and  $MoO_3$  thin films (prepared at room temperature) and correlated the results with other complementary studies of structural, vibrational and surface morphological properties [14].

It may be mentioned that the optical and other physical properties of  $WO_3$  and  $MoO_3$  films strongly depend on their growth temperature [16]. Usually, films grown at higher substrate temperatures offer enhanced optical absorption, optimum stoichiometry, morphology and crystalline alignment. These are the key factors to decide the performance of the films for their suitability in developing special devices. At higher deposition temperatures, the atomic, molecular or ionic species of  $WO_3$  and/or  $MoO_3$  impinged on the substrate surface acquire a large thermal energy and hence a large mobility. As a result, a large number of nuclei are formed which coalesce to form a continuous film with large grains on the substrate. In this work, we have focused on the effects of  $N^+$ -ion irradiation on both  $WO_3$  and  $MoO_3$  films grown at higher temperature (373 K). In particular, changes in the optical property will be correlated with the structural, vibrational and surface morphological properties. In addition, we have addressed a direct comparison of optical data of nitrogen ion irradiated  $WO_3$  and  $MoO_3$  thin films grown at different temperatures.

## 2. Experimental

Thin  $WO_3$  and  $MoO_3$  films were grown on clean Corning 7059 microscopic glass substrates by the electron beam evaporation technique under a chamber pressure of  $1 \times 10^{-5}$  mbar at the substrate temperature ( $T_{\text{sub}}$ ) of 373 K. The thickness of as-grown (pristine)  $WO_3$  and  $MoO_3$  films is 1.28  $\mu\text{m}$  and 1.36  $\mu\text{m}$ , respectively, as observed by *in situ* quartz crystal thickness monitor during evaporation. The films were uniformly irradiated by 2 MeV  $N^+$  ions at room temperature (RT) to the fluences of  $1 \times 10^{12}$ ,  $1 \times 10^{13}$ ,  $1 \times 10^{14}$  and  $1 \times 10^{15}$  ions  $\text{cm}^{-2}$ . All the samples were irradiated with the beam size of  $1 \times 1 \text{ cm}^2$  under secondary electron suppressed geometry. The flux of incident ions was kept low ( $< 10^{10}$  ions  $\text{cm}^{-2} \text{ s}^{-1}$ ) to prevent irradiation induced sample heating. Monte Carlo SRIM-2006 simulation [17] predicts the projected range of the N ion in  $WO_3$  and  $MoO_3$  films to be 1.5  $\mu\text{m}$  and 1.4  $\mu\text{m}$ , respectively, and hence the ions are expected to penetrate into the substrate, thereby transferring energy to the sample via electronic and nuclear loss mechanisms. Thus, any kind of compound formation (in the form of nitride or oxynitride) may be practically excluded within the  $WO_3$  and the  $MoO_3$  films. Such deep penetration of MeV ions also offers the advantage of modifying a thick layer which is less influenced by surface effects. The nuclear energy loss ( $S_n$ ) and the electronic energy loss ( $S_e$ ) values in the  $WO_3$  films are  $1.2 \times 10^{-4}$  keV  $\text{nm}^{-1}$  and  $1.6 \times 10^{-2}$  keV  $\text{nm}^{-1}$ ,

respectively (as obtained from SRIM-2006 simulation), while those for the  $MoO_3$  films are given by  $1.2 \times 10^{-4}$  keV  $\text{nm}^{-1}$  and  $1.9 \times 10^{-2}$  keV  $\text{nm}^{-1}$ , respectively. Since for both types of films, the  $S_n$  values are two orders of magnitude smaller than the  $S_e$  values, the incident nitrogen ions lose energy predominantly via inelastic collisions with the target electrons.

The phase identification of the pristine and the  $N^+$ -ion irradiated films was studied by powder x-ray diffractometry (XRD) with monochromatic Cu  $K\alpha$  radiation source ( $\lambda = 0.154 \text{ nm}$ ) over a  $2\theta$  scan range  $35^\circ$ – $55^\circ$ . Irradiation-induced changes in optical properties of  $WO_3$  and  $MoO_3$  films were studied by using UV–visible (Vis)–near infrared (NIR) spectrophotometer in the range 300–1100 nm. Micro-Raman spectroscopy was employed to measure the vibrational changes in the films before and after irradiation. The spectra were recorded in the backscattering geometry using a 10  $\mu\text{m}$  spot size of  $Ar^+$ -ion laser ( $\lambda = 514.5 \text{ nm}$ ) with a power of 200 mW. Changes in surface morphology of the films were studied by atomic force microscopy (AFM) with silicon nitride cantilever operated in the tapping mode.

## 3. Results and discussion

### 3.1. X-ray diffraction analysis

X-ray diffraction patterns of the pristine and the irradiated  $WO_3$  and  $MoO_3$  films are shown in figures 1(a) and (b), respectively. It is clearly identified from the XRD patterns of the pristine and the irradiated  $WO_3$  and  $MoO_3$  films that they are polycrystalline in nature. Further, the observed interplanar spacings ( $d$ ) of  $WO_3$  and  $MoO_3$  films confirm that they belong to monoclinic [18] and orthorhombic [19] phases, respectively. The calculated  $d$ -values also indicate that no major structural phase change occurs in both types of films due to irradiation even up to the highest fluence of  $1 \times 10^{15}$   $N^+$   $\text{cm}^{-2}$ . Indeed, a small change takes place in the lattice parameters of  $WO_3$  ( $a = 0.730 \text{ nm}$ ,  $b = 0.770 \text{ nm}$  and  $c = 0.772 \text{ nm}$ ) and  $MoO_3$  ( $a = 0.396 \text{ nm}$ ,  $b = 1.385 \text{ nm}$  and  $c = 0.369 \text{ nm}$ ) films irradiated up to the highest fluence [18, 19]. Such a negligible change in the lattice parameters implies only the slight distortion in the W–O and Mo–O frameworks upon  $N^+$ -ion irradiation. However, the increasing peak intensity and decreasing FWHM of the diffraction peaks with increasing ion fluence indicate an irradiation induced grain growth.

This inference is corroborated in figures 2(a) and (b) as an increase in the average crystallite size ( $D$ ) and the decreasing dislocation density ( $\delta$ ) of the predominant peaks (004) and (060) of the  $WO_3$  and  $MoO_3$  films, respectively, with increasing ion fluence. It may be mentioned here that  $D$  is defined as  $0.94\lambda/\beta \cos \theta$  (Scherrer's formula) [20], where  $\beta$  is the full width at half maximum (in radians) of the XRD peak and  $\delta$  is defined as  $1/D^2$  [21]. In addition, new crystalline peaks oriented along the (222) and (040) directions have been observed for  $WO_3$  films after the fluence of  $1 \times 10^{12}$   $N^+$   $\text{cm}^{-2}$  (figure 1(a)). The decrease in dislocation density with increasing ion fluence can be explained as follows: it is obvious that during ion irradiation, two competing processes occur

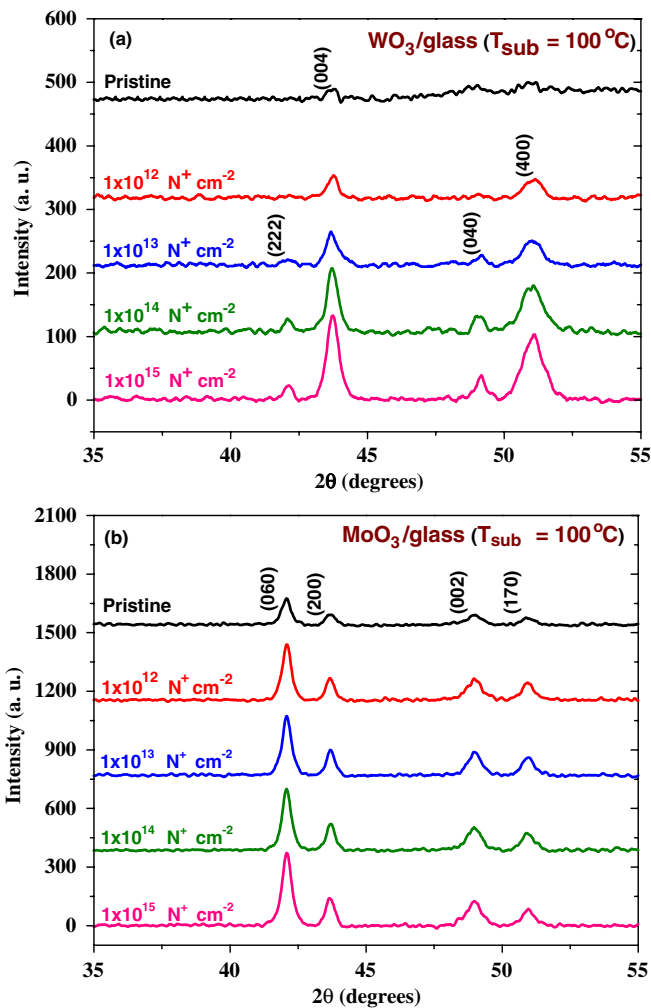


**Figure 1.** (Colour online) X-ray diffraction patterns of (a)  $\text{WO}_3$  and (b)  $\text{MoO}_3$  thin films before and after  $\text{N}^+$ -ion irradiation to various fluences.

simultaneously; (i) the generation of vacancies, agglomeration of vacancies and then collapsing into dislocation loops, (ii) their annihilation at the possible sinks. With increasing ion fluence though more vacancies are created, annihilation rate of vacancies also increases as the sink density increases with irradiation.

### 3.2. Micro-Raman analysis

Figure 3(a) shows the Raman spectra of  $\text{WO}_3$  films before and after nitrogen ion irradiation. Generally  $\text{WO}_3$  has the  $\text{ReO}_3$ -type crystal structure, which is composed of a network of corner-shared  $\text{WO}_6$  octahedron units [22]. These octahedron units are capable of forming clusters having different types of structures: (a) closed, spatial dense-packed structure, (b) closed, planar dense-packed structure and (c) open chain-like structure composed of the ring-membered 3, 4, 5 and 6 octahedrons. These clusters are supposed to be connected to each other by O–W–O grains with terminal W=O bonds at the boundaries [23, 24]. The observed Raman peaks at  $674$  and  $807\text{ cm}^{-1}$  can be interpreted as the symmetric O–W–O stretching mode. It is consistent with the analysis

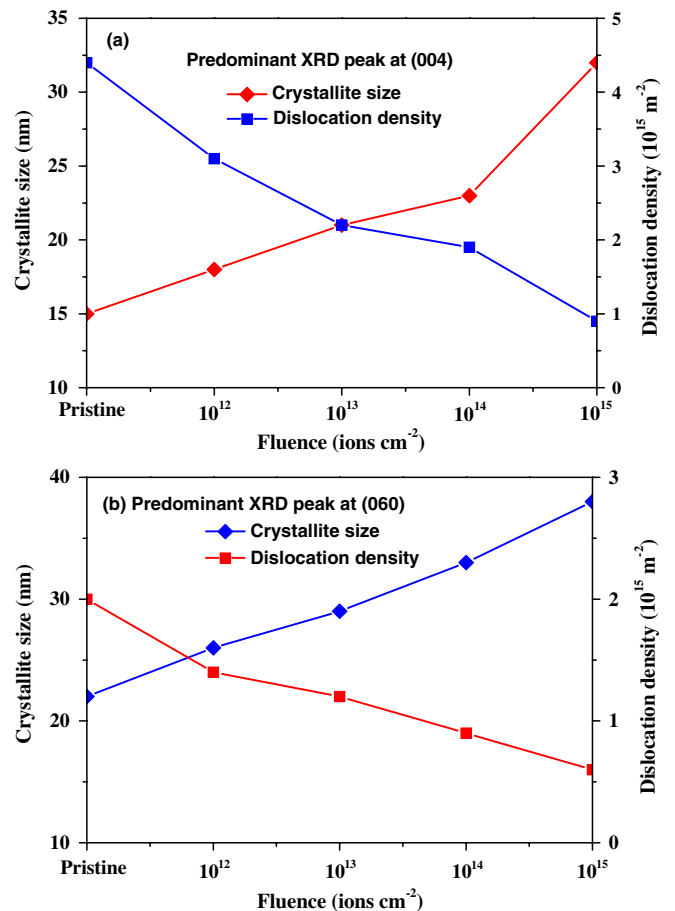


**Figure 2.** (Colour online) Variation in the crystallite size ( $D$ ) and the dislocation density ( $\delta$ ) versus  $\text{N}^+$ -ion fluence for (a)  $\text{WO}_3$  films and (b)  $\text{MoO}_3$  films.

of Raman data for monoclinic  $\text{WO}_3$  films as reported by Daniel *et al* [23] and Haro-Poniatowski *et al* [25]. The peak at  $956\text{ cm}^{-1}$  corresponds to the symmetric W=O stretching mode of terminal oxygen, possibly on the surface of the cluster. It is well formed, but substantially broadened and has effectively disappeared as the ion fluence increases. According to Shigesato *et al* [26], a higher crystallinity of  $\text{WO}_3$  film corresponds to a smaller intensity ratio of the two stretching modes W=O and W–O. As a matter of fact, since there is no possibility of nitride or oxynitride phase formation within the  $\text{WO}_3$  films a decrease in intensity of the W=O peak with increasing ion fluence may be indicative of increasing grain size of the films, which is clearly seen from figure 2(a). Thus, micro-Raman data are consistent with the XRD analysis of the films.

In addition, it can be mentioned here that Kubo and Nishikitani [27] reported that the ratio of integrated Raman scattering intensities of the W=O band to that of the O–W–O band can be employed as a measure of cluster size, and concluded that the quantity of W=O is inversely proportional to the cluster size. Such a correlation is indeed present in our case as well. Moreover, Salje [28] reported a change in the Raman spectra of crystalline tungsten oxide to be caused due to a phase transition, although Shigesato *et al* [26] observed that the location of the Raman peak at  $807\text{ cm}^{-1}$  is hardly affected

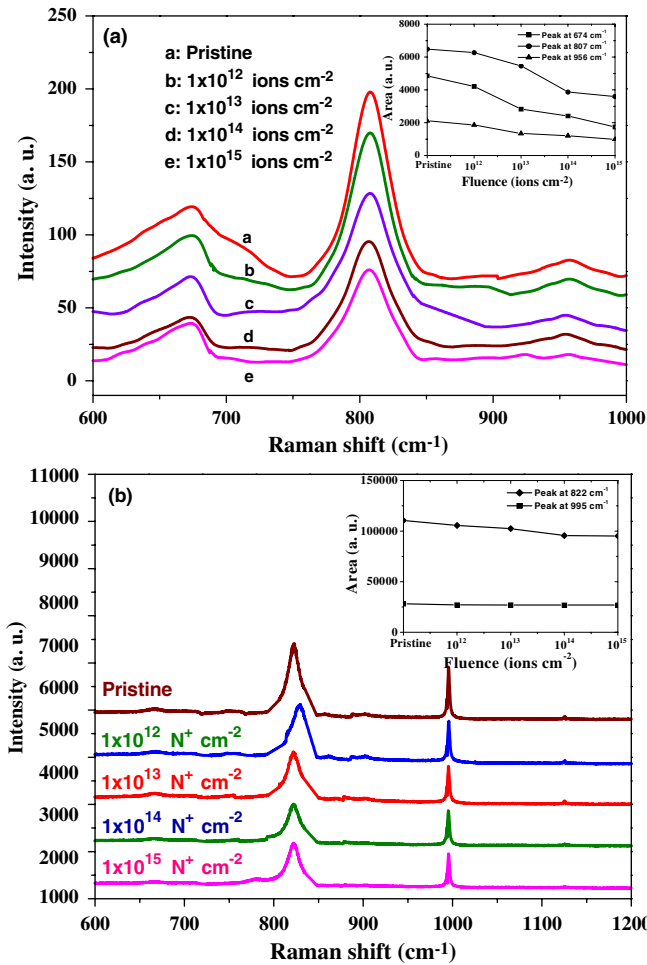


**Figure 3.** (Colour online) Micro-Raman spectra of (a)  $\text{WO}_3$  and (b)  $\text{MoO}_3$  films before and after  $\text{N}^+$ -ion irradiation at various fluences. The insets show the variation in the Raman peak area with ion fluence.

due to the structural phase transition. We do not observe any significant peak shift to take place in Raman spectra of the films due to irradiation, which indicates that no structural phase transition takes place in the  $\text{WO}_3$  films upon ion irradiation. This corroborates our XRD findings described earlier.

The Raman spectra of the pristine and the irradiated  $\text{MoO}_3$  films are shown in figure 3(b). The observed Raman active band at  $995\text{ cm}^{-1}$  corresponds to the stretching mode of the Mo–O and this peak is associated with the unique molybdenyl band, which is responsible for the layered structure of orthorhombic molybdenum oxide ( $\alpha\text{-MoO}_3$ ). The sharp peak at  $822\text{ cm}^{-1}$  is attributed to the stretching vibrations of Mo–O–Mo bonding in  $\alpha\text{-MoO}_3$  [29, 30].

It is clearly seen from figures 3(a) and (b) that the relative intensity of the Raman peaks, as compared with the pristine ones, decreases with increasing ion fluence which is presumably due to the electronic screening of phonons in conjunction with intraband activity within the framework of proposed band structure in the metallic state [15]. However, the small shift in the Raman peak at  $822\text{ cm}^{-1}$  (figure 3(b)) towards the higher wave number could be considered as an experimental artefact whose origin is not clear to us. It can be mentioned here that the area under all the Raman peaks

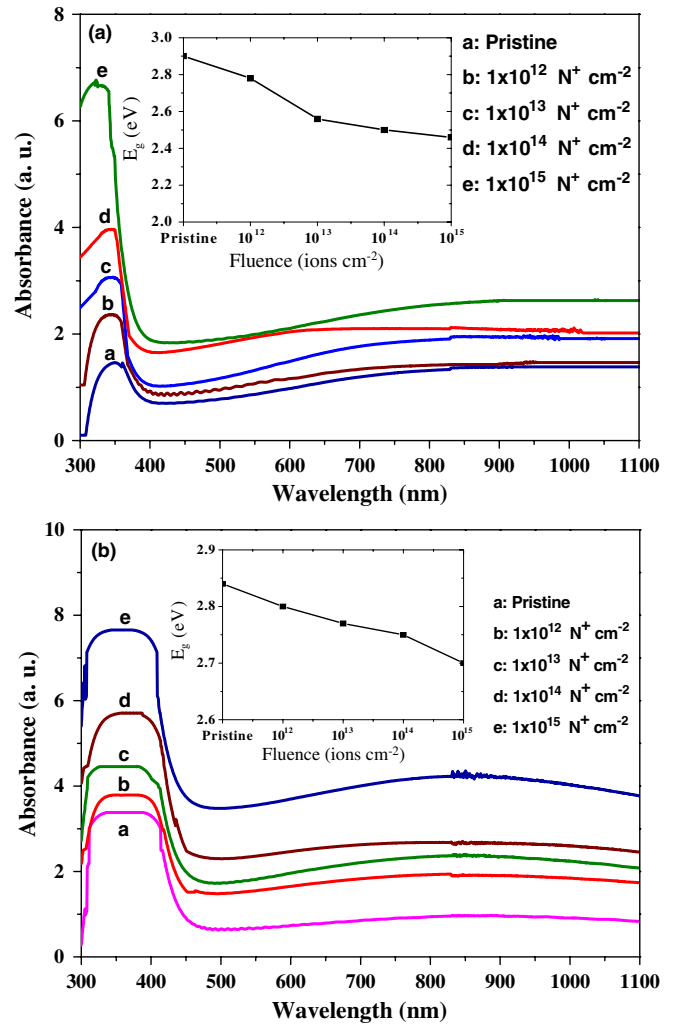


**Figure 4.** (Colour online) Optical absorption spectra of (a)  $\text{WO}_3$  and (b)  $\text{MoO}_3$  films before and after nitrogen irradiation at various fluences. The insets show the variation in the energy band gap of  $\text{WO}_3$  and  $\text{MoO}_3$  films with ion fluence.

decreases with increasing ion fluence, as observed in insets of figures 3(a) and (b), which is attributed to deterioration in the translational symmetry of the  $\text{WO}_3$  and  $\text{MoO}_3$  crystals caused by irradiation induced lattice disorder [31]. This interpretation is consistent with our XRD studies, where we observe an irradiation induced distortion in the W–O and Mo–O frameworks.

### 3.3. Optical and surface morphological properties

Figures 4(a) and (b) show the optical absorption spectra of pristine and irradiated  $\text{WO}_3$  and  $\text{MoO}_3$  films, respectively. A sharp increase in optical absorption is observed with increasing ion fluence, which is caused by free-carrier absorption corresponding to an increase in the conductivity [32, 33]. In addition, it is clear from the spectra that the absorption edges shift towards the higher wavelengths, indicating a systematic reduction in the optical energy band gap,  $E_g$ , of the films with increasing ion fluence, as evident from the insets of figures 4(a) and (b). The observed red-shift in the absorption edges of irradiated films may also be correlated with the coalescence

of small crystallites into effectively larger crystallites (grain growth) but at the same time retaining the nanostructure morphology of the film surfaces. The observed  $E_g$  values (indirect band gap) of  $\text{WO}_3$  films are 2.90 eV, 2.78 eV, 2.56 eV, 2.50 eV and 2.46 eV, respectively, for the pristine and irradiated samples corresponding to fluences of  $1 \times 10^{12}$  ions  $\text{cm}^{-2}$ ,  $1 \times 10^{13}$  ions  $\text{cm}^{-2}$ ,  $1 \times 10^{14}$  ions  $\text{cm}^{-2}$  and  $1 \times 10^{15}$  ions  $\text{cm}^{-2}$ , respectively. On the other hand,  $\text{MoO}_3$  is a direct band gap material and the respective  $E_g$  values corresponding to the above fluences are 2.84 eV, 2.80 eV, 2.77 eV, 2.75 eV and 2.70 eV. This decreasing trend in  $E_g$  indicates that the top of the valence band and the bottom of the conduction band are modified to various extents with increasing ion fluence, which is attributed primarily to the Moss–Burstein shift in semiconductors [34]. In order to have a better insight into the role of growth temperature, we now try to compare the optical data obtained from the present set of  $\text{WO}_3$  and  $\text{MoO}_3$  films (grown at 373 K) with our reported data [14] on the respective films prepared at RT. It is observed that irradiation leads to a larger enhancement in the optical absorption for both  $\text{WO}_3$  and  $\text{MoO}_3$  films prepared at 373 K (as compared with those grown at RT). In addition, we find that the optical energy band gap values of high temperature grown  $\text{WO}_3$  and  $\text{MoO}_3$  films were lower than those of RT prepared films. The band gap narrowing through the substrate temperature revealed the enhancement in crystallization of the films [2].

Further, based on our earlier works [35, 36], the decrease in the energy band gap of  $\text{WO}_3$  films with growing substrate temperature (up to 373 K) was observed to be 88%, while an RT-grown film upon annealing even at 573 K leads to a decrease in the  $E_g$  value by 91% [35]. On the other hand, by irradiating the RT-grown  $\text{WO}_3$  film at the highest fluence ( $1 \times 10^{15}$  ions  $\text{cm}^{-2}$ ) [14], we observe a change in  $E_g$  by 82%, while reduction in the  $E_g$  for 373 K grown  $\text{WO}_3$  film subjected to  $\text{N}^+$ -ion irradiation under similar condition leads to a value of 84%. Likewise,  $\text{MoO}_3$  films grown at RT and at 373 K and later on irradiated by nitrogen ions under similar conditions lead to change in the energy band gap values by 95% and 95%, respectively. Whereas, the  $\text{MoO}_3$  films grown at higher substrate temperature of 373 K and annealing of the RT-grown samples even up to 573 K lead to changes in respective  $E_g$  values only by 89% and 92% [36]. Therefore, for both cases, namely post growth thermal annealing and high temperature growth, the optical band gap of  $\text{WO}_3$  and  $\text{MoO}_3$  films decreases by a significant amount. At the same time, N-ion irradiation also leads to a distinct reduction in the  $E_g$  value. However, the trends are different in the two types of films and there seems to be no correlation between the results obtained by annealing the RT-grown films at higher temperatures and high temperature grown films subjected to N-ion irradiation.

In fact, it was reported [35, 36] that the shrinkage in the values of energy band gap (decrease in  $E_g$ ) from RT to higher substrate temperatures and/or annealing temperatures is caused due to the formation of oxygen-ion vacancies in the films. Later on, this inference was independently corroborated by x-ray photoelectron spectroscopic (XPS) measurements, where the decrease in concentration of oxygen with increasing substrate and annealing temperatures of both  $\text{WO}_3$  and  $\text{MoO}_3$  thin films was observed [5, 6].

It may be mentioned here that ion irradiation produces point defects such as vacancies, antisite defects and interstitials, causing lattice damage. Hence, the reduction in  $E_g$  with increasing ion fluence may arise due to the effect of band tailing, owing to the defects produced during irradiation. In fact, the MeV ions excite the electrons from both the lone pair and bonding states to the higher-energy states. Vacancies created in these states are immediately filled by the outer electrons with Auger processes that, in turn, induce more holes in the lone pair and bonding orbital, leading to a vacancy cascade process. The vacancies occupied by electrons act as donor centres, which are responsible for broad band absorption. These donor centres are in the forbidden gap and form a narrow donor band at about 0.3 eV below the conduction band. Thus, MeV  $\text{N}^+$ -ion induced defects give rise to localized states near the band edge and as a consequence the energy gap of the pristine sample gets modified.

In addition, it can be mentioned here that Senthil *et al* [37] reported that the decrease in the optical energy band gap can be correlated with the reduction in peak area of different Raman lines, which is consistent with our micro-Raman analyses where we observed the decrease in Raman peak area of  $\text{WO}_3$  and  $\text{MoO}_3$  films with increasing ion fluence (insets of figures 3(a) and (b)). Further,  $E_g$  also shows a tendency to decrease when the  $\text{W}=\text{O} : \text{O}-\text{W}-\text{O}$  ratio reduces [27]. This is consistent with our results, yielding a decrease in the  $E_g$  value (inset of figure 4(a)) with decreasing intensity of the  $\text{W}=\text{O}$  band (figure 3(a)).

We also performed surface morphological measurements on nitrogen ion irradiated  $\text{WO}_3$  and  $\text{MoO}_3$  films. Figure 5 shows the three-dimensional AFM images of the pristine and irradiated  $\text{WO}_3$  and  $\text{MoO}_3$  films grown at 373 K. The AFM images of pristine  $\text{WO}_3$  and  $\text{MoO}_3$  films (figures 5(a) and (c)) show a homogeneous surface and an architectural network comprising well resolved and textured grain morphology. When the pristine  $\text{WO}_3$  film is subjected to irradiation at the highest fluence of  $1 \times 10^{15}$  ions  $\text{cm}^{-2}$  (figure 5(b)), the AFM structure may be characterized as small pearl-like grains with bumps originating from the columnar growth of the films that promoted the dense structure, while the irradiated  $\text{MoO}_3$  film (figure 5(d)) shows small spherical wrinkled mountains originating from the columnar growth of the films. The change in surface morphology (AFM features) by the effect of  $\text{N}^+$ -ion irradiation is mainly due to the realization of crystallites of varying crystalline nature and size, which is consistent with our XRD findings where we observe an irradiation induced grain growth.

Further, it is observed that the average root mean square surface roughness ( $R_{\text{rms}}$ ) of the films increases with ion fluence. For example, the  $R_{\text{rms}}$  of pristine  $\text{WO}_3$  and  $\text{MoO}_3$  films are 0.7 nm and 1.8 nm, respectively, which increase up to 1.5 nm and 2.4 nm, respectively, for irradiation at a fluence of  $1 \times 10^{15}$  ions  $\text{cm}^{-2}$ . In order to compare the change in surface morphological properties of N-ion irradiated films due to the effect of growth temperatures, the AFM images of our reported [14] pristine and irradiated  $\text{WO}_3$  films (grown at RT) are given here (figure 6). The  $R_{\text{rms}}$  of pristine and irradiated (at a fluence of  $1 \times 10^{15}$  ions  $\text{cm}^{-2}$ )  $\text{WO}_3$  films grown at RT

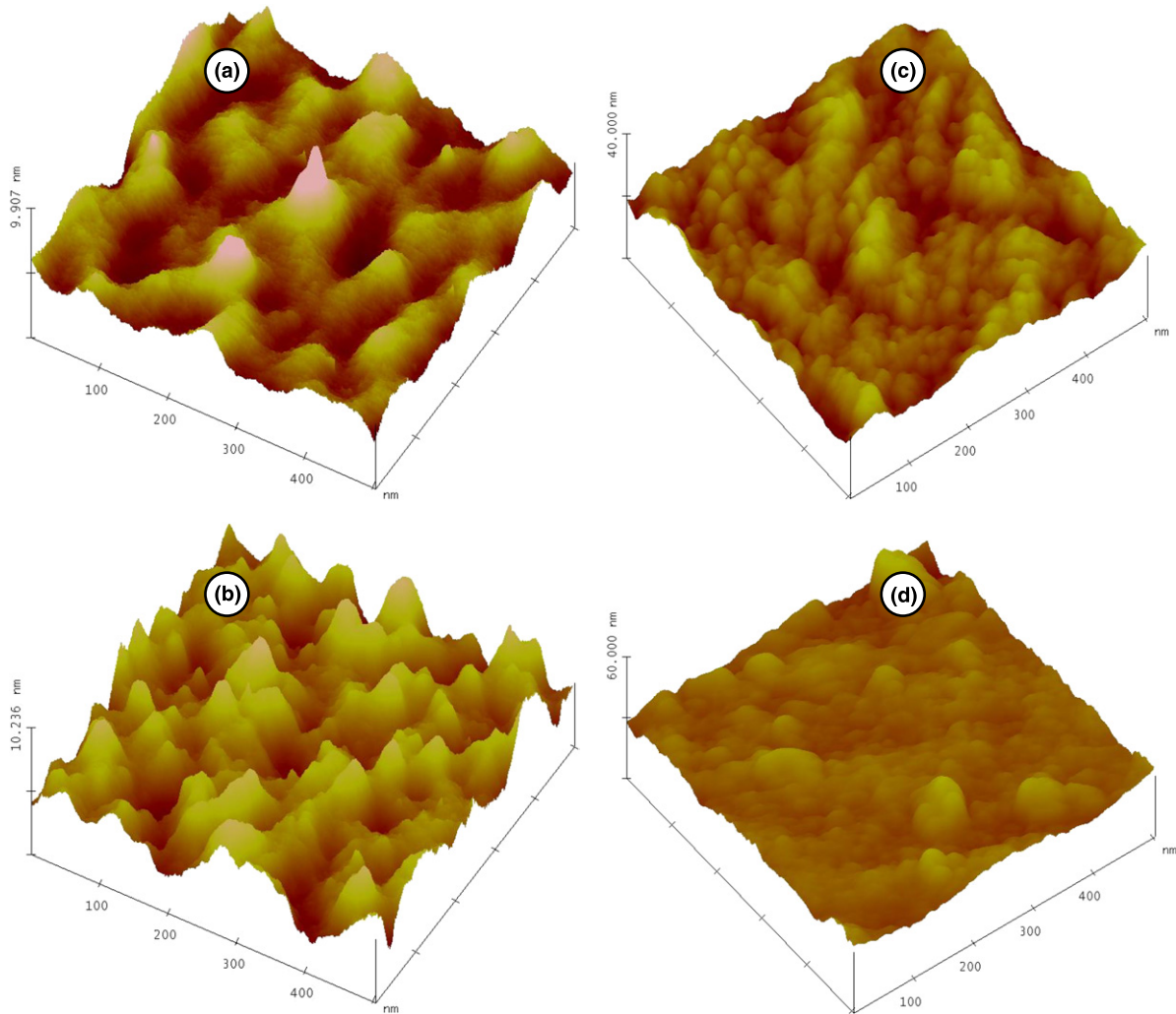


**Figure 5.** (Colour online) AFM images before and after  $N^+$ -ion irradiation: (a) pristine  $WO_3$  film, (b) the same irradiated at a fluence of  $1 \times 10^{15} N^+ cm^{-2}$ , (c) pristine  $MoO_3$  film and (d) the same irradiated at a fluence of  $1 \times 10^{15} N^+ cm^{-2}$ .

are 3.7 nm and 7.4 nm, respectively. The root mean square surface roughness of  $WO_3$  films become less when we grow at 373 K (compared with that grown at RT). In addition, we have estimated the percentage increase in  $R_{rms}$  of  $WO_3$  films when irradiated to the fluence of  $1 \times 10^{15}$  ions  $cm^{-2}$ . For instance,  $R_{rms}$  increases up to 50% upon irradiation of RT-grown  $WO_3$  films, while irradiation induced increase in the film surface roughness is less (46%) in the case of  $WO_3$  films grown at 373 K. Likewise, a similar kind of behaviour is observed for the  $MoO_3$  films grown at RT and 373 K.

It can be mentioned here that the effects of 2 MeV nitrogen ions would be governed by electronic excitation, which is responsible for the changes in the irradiated films. Generally, it is expected that the electronic energy loss will not cause any movement of atoms because it is typically known to cause either excitation or ionization. However,  $WO_3$  and  $MoO_3$  films are insulating in nature and, according to the Coulomb explosion model, the positive charges generated by the incident ions along their paths may cause atomic motion due to the Coulomb force [38]. Therefore, the increasing surface roughness can be attributed to such atomic movements caused due to  $N^+$ -ion irradiation.

#### 4. Summary and conclusions

In summary, we have studied 2 MeV nitrogen ion irradiation induced modifications in the structural, vibrational, optical and surface morphological properties of thin  $WO_3$  and  $MoO_3$  films grown at 373 K. We observe irradiation induced grain growth in both types of films by XRD analysis, although no structural phase transition takes place due to irradiation even up to the maximum fluence of  $1 \times 10^{15} N^+ cm^{-2}$ , which is corroborated by micro-Raman analysis. Further the increasing crystallite size of  $WO_3$  films with ion fluence is correlated with Raman studies, where we observe a decreasing intensity of the Raman peak of  $W=O$  band with increasing ion fluence. The reduction in the Raman active band of  $MoO_3$  films at  $995 cm^{-1}$  is attributed to the destruction of the layered structure in orthorhombic  $MoO_3$ . In addition, the area under the Raman peaks decreases with increasing ion fluence, which is attributed to deterioration of the translational symmetry in both  $WO_3$  and  $MoO_3$  lattices due to irradiation induced defects. This interpretation is consistent with our XRD studies where we observe an irradiation induced distortion in the  $W-O$  and  $Mo-O$  frameworks. Optical studies show an increase in the

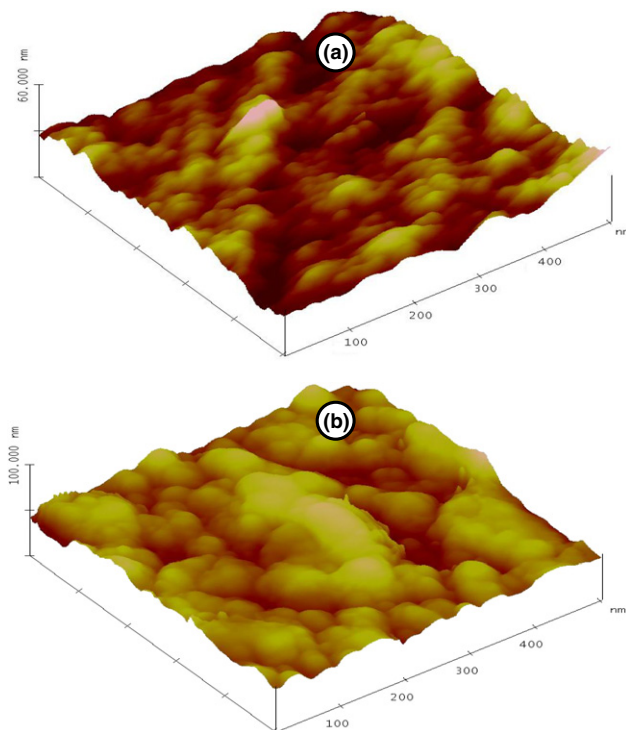


**Figure 6.** (Colour online) AFM images before and after  $N^+$ -ion irradiation to various fluences: (a) RT-grown pristine  $WO_3$  film ( $500\text{ nm} \times 500\text{ nm} \times 60\text{ nm}$ ) and (b) RT-grown  $WO_3$  film irradiated to the fluence of  $1 \times 10^{15}\text{ N}^+\text{ cm}^{-2}$  ( $500\text{ nm} \times 500\text{ nm} \times 100\text{ nm}$ ) [14].

optical absorption and a systematic reduction in the band gap values of both types of films with increasing ion fluence. This is attributed to the nitrogen ion induced defects leading to the production of localized states near the band edges and in the energy gap of  $WO_3$  and  $MoO_3$ . In addition, nitrogen irradiation of high temperature grown  $WO_3$  and  $MoO_3$  films leads to a larger enhancement in optical absorption than films grown at RT. Further, we observe an increasing surface roughness of the films at higher fluences due to irradiation induced atomic motion. Thus, the physical properties of  $WO_3$  or  $MoO_3$  thin films, grown under different conditions, can be tuned by ion irradiation in a controlled manner.

## Acknowledgments

The authors thank the Pelletron group for providing an uninterrupted beam during the irradiation work. S N Sahu is acknowledged for the use of the Raman scattering and optical absorption facilities. Thanks are due to S Varma for the use of the AFM facility.

## References

- [1] Goodenough J B 1990 *Solid State Microbatteries (NATO-ASI Series, Series B vol 209)* ed J R Akridge and M Balkanski (New York: Plenum)
- [2] Julien C, Khelifa A, Hussain O M and Nazri G A 1995 *J. Cryst. Growth* **156** 235
- [3] Donnadiou A 1989 *Mater. Sci. Eng. B* **3** 185
- [4] Pulker H K 1987 *Coating on Glass* (New York: Elsevier)
- [5] Sivakumar R, Gopalakrishnan R, Jayachandran M and Sanjeeviraja C 2006 *Smart Mater. Struct.* **15** 877
- [6] Sivakumar R, Gopinath C S, Jayachandran M and Sanjeeviraja C 2007 *Curr. Appl. Phys.* **7** 76
- [7] Deb S K 1973 *Phil. Mag.* **27** 801
- [8] Goulding M R, Thomas C B and Hurditch R J 1983 *Solid State Commun.* **46** 451
- [9] Papaefthimiou S, Leftheriotis G and Yianoulis P 1998 *Ionics* **4** 321
- [10] Williams J S and Poate J M 1984 *Ion Implantation and Beam Process* (New York: Academic)
- [11] Miyakawa M, Kawamura K, Hosono H and Kawazoe H 1998 *J. Appl. Phys.* **84** 5610
- [12] Crandall R S and Faughnan B W 1977 *Phys. Rev. Lett.* **39** 232
- [13] Wagner W, Rauch F, Feile R, Ottermann C and Bange K 1993 *Thin Solid Films* **235** 228
- [14] Mertz M, Durner R, Heinz B and Ziemann P 2000 *Nucl. Instrum. Methods Phys. Res. A* **166–167** 334
- [15] Mertz M, Eisenmenger J, Heinz B and Ziemann P 2002 *Phys. Rev. B* **66** 184102
- [16] Sivakumar R, Sanjeeviraja C, Jayachandran M, Gopalakrishnan R, Sarangi S N, Paramanik D and Som T 2007 *J. Appl. Phys.* **101** 034913
- [17] Sivakumar R, Sanjeeviraja C, Jayachandran M, Gopalakrishnan R, Sarangi S N, Paramanik D and Som T 2007 *J. Phys.: Condens. Matter* **19** 186204
- [18] Miyakawa M, Ueda K and Hosono H 2002 *J. Appl. Phys.* **92** 2017
- [19] Bunshah R F 1981 *Thin Solid Films* **80** 255
- [20] Julien C, El-Farh L, Balkanski M, Hussain O M and Nazri G A 1993 *Appl. Surf. Sci.* **65–66** 325
- [21] Zeigler J F, Biersack J P and Littmark U 1985 *The Stopping and Ranges of Ions in Solids* vol 1 (New York: Pergamon) <http://www.srim.org/>
- [22] JCPDS 2000 *International Center for Diffraction Data Powder Diffraction File No. 83–0950* (ICDD, Newton Square, PA)
- [23] JCPDS 2000 *International Center for Diffraction Data Powder Diffraction File No. 05–0508* (ICDD, Newton Square, PA)
- [24] Cullity B D 1978 *Element of X-Ray Diffraction* (Philippines: Addison-Wesley)
- [25] Williamson G B and Smallman R C 1956 *Phil. Mag.* **1** 34
- [26] Granqvist C G 1995 *Handbook of Inorganic Electrochromic Materials* (Amsterdam: Elsevier)
- [27] Daniel M F, Desbat B, Lassegues J C, Gerand B and Figlarz M 1987 *J. Solid State Chem.* **67** 235
- [28] Shigesato Y 1991 *Japan. J. Appl. Phys.* **30** 1457
- [29] Haro-Poniatowski E, Jouanne M, Morhange J F, Julien C, Diamant R, Fernandez-Guasti M, Fuentes G A and Alonso J C 1998 *Appl. Surf. Sci.* **127–129** 674
- [30] Shigesato Y, Murayama A, Kamimori T and Matsuhiro K 1988 *Appl. Surf. Sci.* **33–34** 804
- [31] Kubo T and Nishikitani Y 1998 *J. Electrochem. Soc.* **145** 1729
- [32] Salje E 1975 *Acta Crystallogr. A* **31** 360
- [33] Segun L, Figlarz M, Cavagnat R and Lassegues J C 1995 *Spectrochim. Acta A* **51** 1323
- [34] Gesheva K A, Ivanova T and Hamelmann F 2006 *Sol. Energy Mater. Sol. Cells* **90** 2532
- [35] Motooka T and Holland O W 1992 *Appl. Phys. Lett.* **61** 3005
- [36] Svensson J S E M and Granqvist C G 1984 *Appl. Phys. Lett.* **45** 828
- [37] Tate T J, Garcia-Parajo M and Green M 1991 *J. Appl. Phys.* **70** 3509
- [38] Ramamoorthy K, Sanjeeviraja C, Jayachandran M, Sankaranarayanan K, Misra P and Kukreja L M 2006 *Curr. Appl. Phys.* **6** 103

- [35] Sivakumar R, Jayachandran M and Sanjeeviraja C 2004 *Mater. Chem. Phys.* **87** 439  
Sivakumar R, Gopalakrishnan R, Jayachandran M and Sanjeeviraja C 2007 *Opt. Mater.* **29** 679
- [36] Sivakumar R, Gopalakrishnan R, Jayachandran M and Sanjeeviraja C 2007 *Curr. Appl. Phys.* **7** 51
- Sivakumar R, Jayachandran M and Sanjeeviraja C 2004 *Surf. Eng.* **20** 385
- [37] Senthil K, Mangalaraj D, Narayandass Sa K, Hong B, Roh Y, Park C S and Yi Y 2002 *Semicond. Sci. Technol.* **17** 97
- [38] Fleischer R L, Price P B and Walker R M 1965 *J. Appl. Phys.* **36** 3645